

Effect of a resistive vacuum vessel on dynamo mode rotation in reversed field pinches

R. Fitzpatrick

Institute for Fusion Studies, Department of Physics, University of Texas at Austin, Austin, Texas 78712

S. C. Guo

Consorzio RFX, Corso Stati Uniti 4, 35127 Padova, Italy

D. J. Den Hartog and C. C. Hegna

Department of Physics, University of Wisconsin, Madison, Wisconsin 53706

(Received 6 April 1999; accepted 10 June 1999)

Locked (i.e., nonrotating) dynamo modes give rise to a serious edge loading problem during the operation of high current reversed field pinches. Rotating dynamo modes generally have a far more benign effect. A simple analytic model is developed in order to investigate the slowing down effect of electromagnetic torques due to eddy currents excited in the vacuum vessel on the rotation of dynamo modes in both the Madison Symmetric Torus (MST) [Fusion Technol. **19**, 131 (1991)] and the Reversed Field Experiment (RFX) [Fusion Eng. Des. **25**, 335 (1995)]. This model strongly suggests that vacuum vessel eddy currents are the primary cause of the observed lack of mode rotation in RFX. The eddy currents in MST are found to be too weak to cause a similar problem. The crucial difference between RFX and MST is the presence of a thin, highly resistive vacuum vessel in the former device. The MST vacuum vessel is thick and highly conducting. Various locked mode alleviation methods are discussed. © 1999 American Institute of Physics. [S1070-664X(99)01610-9]

I. INTRODUCTION

A reversed field pinch (or RFP) is a magnetic fusion device which is similar to a tokamak¹ in many ways. Like a tokamak, the plasma is confined by a combination of a toroidal magnetic field, B_ϕ , and a poloidal magnetic field, B_θ , in an axisymmetric toroidal configuration.² Unlike a tokamak, where $B_\phi \gg B_\theta$, the toroidal and poloidal field strengths are comparable, and the RFP toroidal field is largely generated by currents flowing within the plasma. The RFP concept derives its name from the fact that the toroidal magnetic field spontaneously reverses direction in the outer regions of the plasma. This reversal is a consequence of relaxation to a minimum energy state driven by intense magnetohydrodynamical (MHD) mode activity during the plasma start-up phase.³ Intermittent, relatively low-level, mode activity maintains the reversal, by dynamo action, throughout the duration of the plasma discharge. As a magnetic fusion concept, the RFP has a number of possible advantages relative to the tokamak. The magnetic field strength at the coils is relatively low, allowing the possibility of a copper-coil, as opposed to a superconducting-coil, reactor. Furthermore, the plasma current can, in principle, be increased sufficiently to allow ohmic ignition, thus negating the need for auxiliary heating systems.

A conventional RFP plasma is surrounded by a close-fitting, thick, conducting shell whose L/R time is much longer than the duration of the discharge. Such a shell is necessary in order to stabilize external kink modes which would otherwise rapidly destroy the plasma.⁴ In the presence of the shell, the dominant MHD modes are $m=1$ tearing

modes resonant in the plasma core. These modes possess a range of toroidal mode numbers, characterized by $n \sim 2R_0/a$. Here, m, n are poloidal and toroidal mode numbers, respectively, whereas a and R_0 are the minor and major radii of the plasma, respectively. The core tearing modes are responsible for the dynamo action which maintains the field reversal, and are, therefore, generally known as dynamo modes.⁵

The Madison Symmetric Torus (MST)⁶ and the Reversed Field Experiment (RFX)⁷ are both large RFP experiments of broadly similar size and achieved plasma parameters. Nevertheless, the observed dynamics of dynamo modes in these two devices is strikingly different.

In MST, the dynamo modes generally rotate, forming a toroidally localized, phase-locked structure, known as a "slinky mode,"⁸ which also rotates and extends over about one-fourth of the torus.⁹ The dynamo modes continually execute a so-called sawtooth cycle, in which their typical amplitude gradually increases from a small value, until a critical amplitude is reached at which a rapid global magnetic reconnection event, known as a sawtooth crash, is triggered. After the crash, the mode amplitudes return to their initial values, and the process continues ad infinitum. Note that the dynamo action which maintains the field reversal is only significant during the sawtooth crashes. The rotation of the dynamo modes is briefly arrested at each sawtooth crash, but generally resumes afterward. However, in a small fraction of plasma discharges the dynamo modes fail to re-rotate after the crash, setting in train a series of events which eventually leads to the premature termination of the discharge.⁹ The percentage of discharges in which this occurs is a sensitive

function of the plasma parameters and the wall conditioning, but generally increases with increasing plasma current.

In RFX, the dynamo modes form a toroidally localized “slinky mode” which locks to the shell (along with the constituent dynamo modes) during the plasma start-up phase and remains locked, and, therefore, nonrotating, throughout the duration of the discharge.¹⁰ The stationary “slinky mode” does not significantly (i.e., by more than a factor 2, say) degrade the overall plasma confinement,¹¹ but gives rise to a toroidally localized, stationary “hot spot” on the plasma facing surface, presumably because the radial transport due to the diffusion of chaotic magnetic field lines peaks at the toroidal angle where the amplitude of the “slinky mode” attains its maximum value. If the plasma current is made sufficiently large, this “hot spot” overheats the facing surface, leading to the influx of impurities into the plasma, and the eventual termination of the discharge. Indeed, the maximum achievable plasma current in RFX is limited by this effect. Similar edge loading problems are not observed on MST, presumably because the “hot spot” associated with the “slinky mode” rotates (since the constituent dynamo modes rotate).

It is clear, from the above discussion, that the occurrence of severe edge loading problems in RFX, and the relative absence of such problems in MST, is a consequence of the fact that dynamo modes are generally stationary in RFX but usually rotate in MST. Note that other RFPs, in particular the Toroidal Pinch eXperiment-RX (TPE-RX) device,^{12,13} exhibit edge loading problems, associated with locked dynamo modes, which are similar to those observed on RFX. Two possible explanations have been proposed for the lack of mode rotation in RFX. The first explanation focuses on the fact that the stabilizing shell is (relatively speaking) farther away from the plasma in RFX than in MST. This can be expected to destabilize the dynamo modes in RFX, relative to those in MST, thereby increasing their saturated amplitude, and, hence, making them more prone to lock to stray error fields. (Note that the error fields in RFX are only slightly larger than those in MST. Moreover, the error fields in TPE-RX are undoubtedly much less than those in MST. Hence, the different dynamo mode dynamics observed on MST, RFX, and TPE-RX cannot be explained in terms of the intrinsic error-field levels in these devices.) However, this effect is thought to be too weak to account for the observed difference in dynamo mode dynamics between MST and RFX.¹⁴ The second explanation focuses on the fact that in MST the conducting shell is also the vacuum vessel, whereas in RFX a thin resistive vacuum vessel is located between the shell and the edge of the plasma. In tokamaks, it is well-known that eddy currents induced in a resistive vacuum vessel can effectively arrest mode rotation, provided that the mode amplitude becomes sufficiently large.¹⁵ In this paper, we investigate whether similar eddy currents induced in the RFX vacuum vessel can account for the absence of mode rotation in this device (and the presence of mode rotation in MST).

The model adopted in this paper is rather simplistic. Instead of considering a range of unstable $m=1$ modes, we concentrate on the dynamics of a single representative dy-

namo mode in the presence of a thin resistive vacuum vessel surrounded by a thick conducting shell. Furthermore, we only consider zero- β , large aspect-ratio plasmas. Nevertheless, we believe that our model is sufficiently realistic to allow us to determine whether vacuum vessel eddy currents can account for the observed difference in dynamo mode dynamics between RFX and MST.

II. PRELIMINARY ANALYSIS

A. The plasma equilibrium

Consider a large aspect-ratio,¹⁶ zero- β ,¹⁷ RFP plasma equilibrium whose unperturbed magnetic flux-surfaces map out (almost) concentric circles in the poloidal plane. Such an equilibrium is well approximated as a periodic cylinder. Suppose that the minor radius of the plasma is a . Standard cylindrical polar coordinates (r, θ, z) are adopted. The system is assumed to be periodic in the z -direction, with periodicity length $2\pi R_0$, where R_0 is the simulated major radius of the plasma. It is convenient to define a simulated toroidal angle $\phi = z/R_0$.

The equilibrium magnetic field is written

$$\mathbf{B} = [0, B_\theta(r), B_\phi(r)]. \quad (1)$$

The model RFP equilibrium adopted in this paper is the well-known $\alpha - \Theta_0$ model,¹⁸ according to which

$$\nabla \wedge \mathbf{B} = \sigma(r)\mathbf{B}, \quad (2)$$

where

$$\sigma = \left(\frac{2\Theta_0}{a} \right) \left[1 - \left(\frac{r}{a} \right)^\alpha \right]. \quad (3)$$

Here, Θ_0 and α are positive constants.

It is conventional² to parameterize RFP equilibria in terms of the pinch parameter,

$$\Theta = \frac{B_\theta(a)}{\langle B_\phi \rangle}, \quad (4)$$

and the reversal parameter,

$$F = \frac{B_\phi(a)}{\langle B_\phi \rangle}, \quad (5)$$

where $\langle \dots \rangle$ denotes a volume average.

B. Outline of the problem

Suppose that the plasma is surrounded by a concentric, thin, resistive vacuum vessel of minor radius b . The vacuum vessel is, in turn, surrounded by a concentric, perfectly conducting shell of minor radius c . The arrangement of conducting shells surrounding the plasma is illustrated in Fig. 1. This paper investigates the effect of any helical eddy currents excited in the vacuum vessel on the rotation of a typical core tearing mode: the m, n mode, say. All other modes in the plasma are ignored, for the sake of simplicity.

C. The perturbed magnetic field

The magnetic perturbation associated with the m, n tearing mode can be written

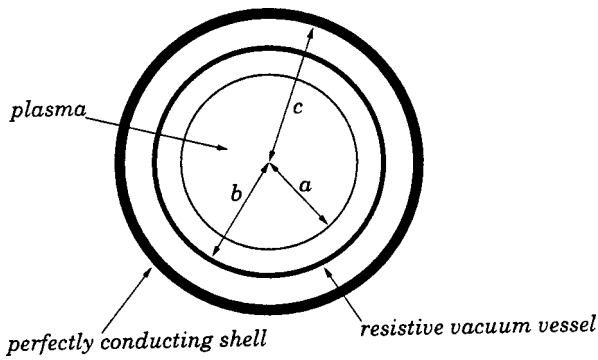


FIG. 1. The arrangement of conducting shells surrounding the plasma.

$$\mathbf{b}(r) = \mathbf{b}^{m,n}(r)e^{i(m\theta - n\phi)}, \tag{6}$$

where m and n are poloidal and toroidal mode numbers, respectively, and

$$b_r^{m,n} = \frac{i\psi^{m,n}}{r}, \tag{7}$$

$$b_\theta^{m,n} = -\frac{m(\psi^{m,n})'}{m^2 + n^2\epsilon^2} + \frac{n\epsilon\sigma\psi^{m,n}}{m^2 + n^2\epsilon^2}, \tag{8}$$

$$b_\phi^{m,n} = \frac{n\epsilon(\psi^{m,n})'}{m^2 + n^2\epsilon^2} + \frac{m\sigma\psi^{m,n}}{m^2 + n^2\epsilon^2}. \tag{9}$$

Here, ' denotes d/dr . Furthermore,

$$\epsilon(r) = \frac{r}{R_0}. \tag{10}$$

In this paper it is assumed that $m \geq 0$.

The linearized magnetic flux function $\psi^{m,n}(r)$ satisfies Newcomb's equation,¹⁹

$$\frac{d}{dr} \left[f^{m,n} \frac{d\psi^{m,n}}{dr} \right] - g^{m,n} \psi^{m,n} = 0, \tag{11}$$

where

$$f^{m,n}(r) = \frac{r}{m^2 + n^2\epsilon^2}, \tag{12}$$

$$g^{m,n}(r) = \frac{1}{r} + \frac{r(n\epsilon B_\theta + mB_\phi)}{(m^2 + n^2\epsilon^2)(mB_\theta - n\epsilon B_\phi)} \frac{d\sigma}{dr} + \frac{2mn\epsilon\sigma}{(m^2 + n^2\epsilon^2)^2} - \frac{r\sigma^2}{m^2 + n^2\epsilon^2}. \tag{13}$$

As is well-known, Eq. (11) is singular at the m/n rational surface, minor radius $r_s^{m,n}$, which satisfies

$$mB_\theta(r_s^{m,n}) - nB_\phi(r_s^{m,n}) = 0. \tag{14}$$

In the vacuum region ($\sigma=0$) surrounding the plasma, the most general solution to Newcomb's equation takes the form

$$\psi^{m,n} = Ai_m(n\epsilon) + Bk_m(n\epsilon), \tag{15}$$

where A, B are arbitrary constants, and

$$i_m(n\epsilon) = |n\epsilon|I_{m+1}(|n\epsilon|) + mI_m(|n\epsilon|), \tag{16}$$

$$k_m(n\epsilon) = -|n\epsilon|K_{m+1}(|n\epsilon|) + mK_m(|n\epsilon|). \tag{17}$$

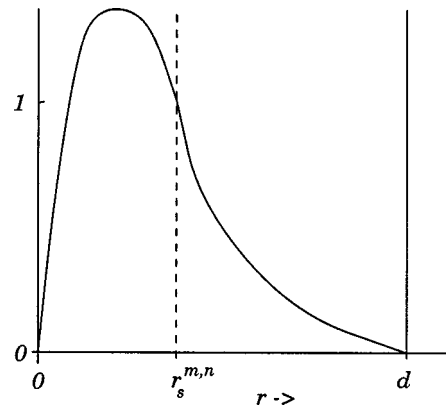


FIG. 2. A typical normalized m,n tearing eigenfunction, $\hat{\psi}_s^{m,n}(r,d)$, calculated assuming the presence of a perfectly conducting shell at minor radius d .

Here, I_m, K_m represent standard modified Bessel functions. For the special case $n=0$, the most general vacuum solution is written

$$\psi^{m,0} = A\epsilon^m + B\epsilon^{-m}. \tag{18}$$

D. Standard tearing eigenfunctions

Let

$$\hat{\psi}_s^{m,n}(r,d) \tag{19}$$

represent the normalized m,n tearing eigenfunction calculated assuming the presence of a perfectly conducting shell at minor radius d . In other words, $\hat{\psi}_s^{m,n}(r,d)$ is a real solution to Newcomb's equation (11) which is well behaved as $r \rightarrow 0$, and satisfies

$$\hat{\psi}_s^{m,n}(r_s^{m,n}, d) = 1, \tag{20}$$

$$\hat{\psi}_s^{m,n}(d, d) = 0. \tag{21}$$

It is easily demonstrated that $\hat{\psi}_s^{m,n}(r,d)$ is zero in the region $r > d$. In general, $\hat{\psi}_s^{m,n}(r,d)$ possesses gradient discontinuities at $r = r_s^{m,n}$ and $r = d$. The quantity

$$E^{m,n}(d) = \left[r \frac{d\hat{\psi}_s^{m,n}(r,d)}{dr} \right]_{r_s^{m,n}-}^{r_s^{m,n}+} \tag{22}$$

can be identified as the standard m,n tearing stability index,²⁰ calculated assuming the presence of a perfectly conducting shell at minor radius d . A typical tearing eigenfunction, $\hat{\psi}_s^{m,n}(r,d)$, is sketched in Fig. 2.

E. Modified tearing eigenfunctions

In the presence of a resistive vacuum vessel, minor radius b , and a perfectly conducting shell, minor radius c , the most general m,n tearing eigenfunction is written

$$\psi^{m,n}(r) = \Psi_s^{m,n} \hat{\psi}_s^{m,n}(r,b) + \Psi_b^{m,n} \hat{\psi}_b^{m,n}(r,b,c), \tag{23}$$

where $\Psi_s^{m,n}$ and $\Psi_b^{m,n}$ are complex parameters which determine the amplitude and phase of the m,n tearing perturbation at the rational surface and vacuum vessel, respectively.

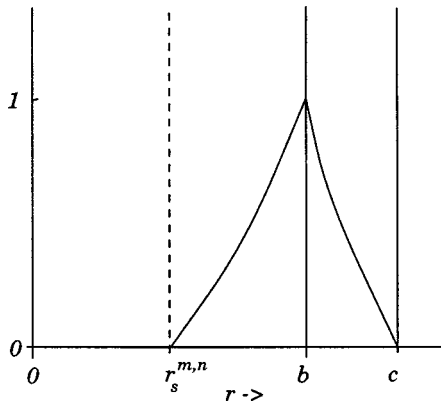


FIG. 3. A typical normalized m,n interaction eigenfunction, $\hat{\psi}_b^{m,n}(r,b,c)$. This eigenfunction parameterizes the interaction between the m,n tearing mode and any eddy currents flowing in the resistive vacuum vessel, minor radius b , in the presence of a perfectly conducting shell of minor radius c .

Note that $\hat{\psi}_b^{m,n}(r,b,c)$ is a real solution to Newcomb's equation which is well behaved as $r \rightarrow 0$, and satisfies

$$\hat{\psi}_b^{m,n}(r_s^{m,n}, b, c) = 0, \tag{24}$$

$$\hat{\psi}_b^{m,n}(b, b, c) = 1, \tag{25}$$

$$\hat{\psi}_b^{m,n}(c, b, c) = 0. \tag{26}$$

It is easily demonstrated that $\hat{\psi}_b^{m,n}(r,b,c)$ is only nonzero for r in the range $r_s^{m,n} < r < c$. In general, $\hat{\psi}_b^{m,n}(r,b,c)$ possesses gradient discontinuities at $r = r_s^{m,n}$, $r = b$, and $r = c$. A typical interaction eigenfunction, $\hat{\psi}_b^{m,n}(r,b,c)$, which parameterizes the interaction between the m,n tearing mode and any eddy currents flowing in the resistive vacuum vessel, minor radius b , in the presence of a perfectly conducting shell of minor radius c , is sketched in Fig. 3.

F. The modified tearing dispersion relation

The dispersion relation for the m,n tearing mode in the presence of the resistive vacuum vessel and perfectly conducting shell takes the form

$$\hat{\psi}_s^{m,n}(r,b) = \begin{cases} \hat{\psi}_s^{m,n}(a,b) \frac{k_m(n\epsilon_b)i_m(n\epsilon) - k_m(n\epsilon)i_m(n\epsilon_b)}{k_m(n\epsilon_b)i_m(n\epsilon_a) - k_m(n\epsilon_a)i_m(n\epsilon_b)} & a \leq r \leq b \\ 0 & r > b \end{cases}, \tag{35}$$

where $\epsilon_a = a/R_0$. It follows from Eqs. (32) and (33) that

$$E_{bs}^{m,n} = \frac{\hat{\psi}_s^{m,n}(a,b)(m^2 + n^2\epsilon_b^2)}{k_m(n\epsilon_b)i_m(n\epsilon_a) - k_m(n\epsilon_a)i_m(n\epsilon_b)}, \tag{36}$$

$$E_{sb}^{m,n} = \frac{\hat{\psi}_s^{m,n}(a,b)(m^2 + n^2\epsilon_s^2)}{k_m(n\epsilon_b)i_m(n\epsilon_a) - k_m(n\epsilon_a)i_m(n\epsilon_b)}. \tag{37}$$

For the special case $n = 0$,

$$\Delta \Psi_s^{m,n} = E^{m,n}(b)\Psi_s^{m,n} + E_{sb}^{m,n}\Psi_b^{m,n}, \tag{27}$$

$$\Delta \Psi_b^{m,n} = -\frac{E_{sb}^{m,n}E_{bs}^{m,n}}{E^{m,n}(c) - E^{m,n}(b)}\Psi_b^{m,n} + E_{bs}^{m,n}\Psi_s^{m,n}, \tag{28}$$

where

$$\Delta \Psi_s^{m,n} = \left[r \frac{d\psi^{m,n}}{dr} \right]_{r_s^{m,n}-}^{r_s^{m,n}+} \tag{29}$$

is a complex parameter which determines the amplitude and phase of the m,n eddy currents flowing in the vicinity of the m,n rational surface, whereas

$$\Delta \Psi_b^{m,n} = \left[r \frac{d\psi^{m,n}}{dr} \right]_{b-}^{b+} \tag{30}$$

is a complex parameter which determines the amplitude and phase of the m,n eddy currents flowing in the vacuum vessel. Furthermore,

$$E_{sb}^{m,n} = \left(r \frac{d\hat{\psi}_b^{m,n}(r,b,c)}{dr} \right)_{r_s^{m,n}+} \tag{31}$$

and

$$E_{bs}^{m,n} = -\left(r \frac{d\hat{\psi}_s^{m,n}(r,b)}{dr} \right)_{b-} \tag{32}$$

are both real parameters.

It is easily demonstrated from Newcomb's equation (11) that

$$(m^2 + n^2\epsilon_b^2)E_{sb}^{m,n} = (m^2 + n^2\epsilon_s^2)E_{bs}^{m,n}, \tag{33}$$

where $\epsilon_b = b/R_0$ and $\epsilon_s = r_s^{m,n}/R_0$. It is also easily demonstrated that

$$\hat{\psi}_b^{m,n}(r,b,c) = \frac{E_{sb}^{m,n}}{E^{m,n}(c) - E^{m,n}(b)} \{ \hat{\psi}_s^{m,n}(r,c) - \hat{\psi}_s^{m,n}(r,b) \}. \tag{34}$$

In the vacuum region outside the plasma

$$E_{bs}^{m,0} = E_{sb}^{m,0} = m \hat{\psi}_s^{m,0}(a,b) \frac{b^{2m} + a^{2m}}{b^{2m} - a^{2m}}. \tag{38}$$

It is clear, from the above analysis, that all of the real parameters appearing in the modified m,n tearing dispersion relation (27)–(28) [i.e., $E^{m,n}(b)$, $E^{m,n}(c)$, $E_{bs}^{m,n}$, $E_{sb}^{m,n}$] can be calculated from a knowledge of the standard tearing eigenfunction $\hat{\psi}_s^{m,n}(r,d)$.

G. Shell physics

Suppose that the vacuum vessel is of radial thickness δ_b and conductivity σ_b . The time constant of the vessel is defined

$$\tau_b = \mu_0 \sigma_b \delta_b b. \quad (39)$$

Adopting the thin-shell approximation, in which it is assumed that there is virtually no radial variation of the tearing eigenfunction $\hat{\psi}^{m,n}(r)$ across the vessel, the dispersion relation of the vacuum vessel takes the form

$$\Delta \Psi_b^{m,n} = i n \Omega_s \tau_b \Psi_b^{m,n}. \quad (40)$$

Here, it is assumed that the m,n tearing mode is saturated (i.e., its amplitude is fixed) and co-rotates with the plasma at its associated rational surface. The plasma is assumed to rotate in the toroidal direction only, for the sake of simplicity. Although the poloidal rotation in RFPs is generally nonzero, it is usually smaller than the toroidal rotation, so its neglect is unlikely to dramatically change any of the results obtained in this paper. In the above,

$$\Omega_s = \Omega(r_s^{m,n}) \quad (41)$$

is the toroidal angular velocity of the plasma at the m,n rational surface, and $\Omega(r)$ is the plasma toroidal angular velocity profile. Note that the thin-shell approximation is valid provided

$$\frac{\delta_b}{b} \ll n \Omega_s \tau_b \ll \frac{b}{\delta_b}. \quad (42)$$

Equations (27), (28), and (40) yield

$$\Delta \Psi_s^{m,n} = \left\{ E^{m,n}(b) + \frac{[E^{m,n}(c) - E^{m,n}(b)]}{1 + i \lambda^{m,n}} \right\} \Psi_s^{m,n}, \quad (43)$$

where

$$\lambda^{m,n} = \frac{n \Omega_s \tau_b [E^{m,n}(c) - E^{m,n}(b)]}{E_{sb}^{m,n} E_{bs}^{m,n}}. \quad (44)$$

The thin-shell approximation is valid provided that

$$\lambda^{m,n} \ll \lambda_c^{m,n}, \quad (45)$$

where

$$\lambda_c^{m,n} = \frac{b}{\delta_b} \frac{[E^{m,n}(c) - E^{m,n}(b)]}{E_{sb}^{m,n} E_{bs}^{m,n}}. \quad (46)$$

H. Electromagnetic torques

The toroidal electromagnetic slowing down torque acting in the vicinity of the m,n rational surface due to eddy currents flowing in the vacuum vessel is given by⁸

$$\delta T_{\phi EM}^{m,n} = \frac{2 \pi^2 R_0}{\mu_0} \frac{n}{m^2 + n^2 \epsilon_s^2} \text{Im} \{ \Delta \Psi_s^{m,n} (\Psi_s^{m,n})^* \}. \quad (47)$$

It follows from Eq. (43) that

$$\begin{aligned} \delta T_{\phi EM}^{m,n} = & - \frac{2 \pi^2 R_0}{\mu_0} \frac{n |\Psi_s^{m,n}|^2}{m^2 + n^2 \epsilon_s^2} \frac{\lambda^{m,n}}{1 + (\lambda^{m,n})^2} \\ & \times [E^{m,n}(c) - E^{m,n}(b)]. \end{aligned} \quad (48)$$

I. Viscous torques

The change in the plasma toroidal angular velocity induced by the electromagnetic slowing down torque is written

$$\Delta \Omega(r) = \Delta \Omega_s \begin{cases} \int_r^a \frac{dr}{r \mu} / \int_{r_s^{m,n}}^a \frac{dr}{r \mu} & r_s^{m,n} \leq r \leq a \\ 1 & r < r_s^{m,n} \end{cases}, \quad (49)$$

where $\mu(r)$ is the plasma (perpendicular) viscosity profile, and

$$\Delta \Omega_s = \Omega_s - \Omega_s^{(0)}. \quad (50)$$

Here, $\Omega_s^{(0)}$ is the value of Ω_s in the absence of eddy currents flowing in the vacuum vessel. In the above, it is assumed that the edge plasma rotation is unaffected by the electromagnetic slowing down torque [i.e., $\Delta \Omega(a) = 0$]. The assumptions underlying the analysis in this section are described in more detail in Ref. 21. Note, in particular, that it is possible to generalize the analysis to take account of the fact that tearing modes do not generally co-rotate with the ion fluid in RFPs without significantly changing any of the results obtained in this paper.

The viscous restoring torque acting in the vicinity of the rational surface is written

$$\delta T_{\phi VS}^{m,n} = 4 \pi^2 R_0 \left[r \mu R_0^2 \frac{d \Delta \Omega}{dr} \right]_{r_s^{m,n}}^{r_s^{m,n}+}. \quad (51)$$

It follows from Eqs. (49) and (50) that

$$\delta T_{\phi VS}^{m,n} = 4 \pi^2 R_0^3 [\Omega_s^{(0)} - \Omega_s] \int_{r_s^{m,n}}^a \frac{dr}{r \mu}. \quad (52)$$

J. Torque balance

Torque balance in the vicinity of the rational surface requires that

$$\delta T_{\phi EM}^{m,n} + \delta T_{\phi VS}^{m,n} = 0. \quad (53)$$

It follows from Eqs. (48) and (52) that

$$\left(\frac{b_s^{m,n}}{\Lambda B_0} \right)^2 \frac{\lambda^{m,n}}{1 + (\lambda^{m,n})^2} = \lambda_{(0)}^{m,n} - \lambda^{m,n}, \quad (54)$$

where

$$\lambda_{(0)}^{m,n} = \frac{n \Omega_s^{(0)} \tau_b [E^{m,n}(c) - E^{m,n}(b)]}{E_{sb}^{m,n} E_{bs}^{m,n}}, \quad (55)$$

B_0 is a typical equilibrium magnetic field strength,

$$b_s^{m,n} = \frac{|\Psi_s^{m,n}|}{r_s^{m,n}} \quad (56)$$

is the perturbed radial magnetic field strength at the m,n rational surface,

$$\tau_H = \frac{\sqrt{\mu_0 \rho_0} a}{B_0} \quad (57)$$

is a typical hydromagnetic time scale,

$$\tau_V = \frac{\rho_0 a^2}{\mu(0)} \tag{58}$$

is a typical viscous diffusion time scale, ρ_0 is the central plasma mass density, and

$$\Lambda = \left[2 \frac{\tau_H^2}{\tau_b \tau_V} \frac{m^2 + n^2 \epsilon_s^2}{n^2 \epsilon_s^2} \frac{E_{sb}^{m,n} E_{bs}^{m,n}}{[E^{m,n}(c) - E^{m,n}(b)]^2} \right]^{1/2} \int_{r_s^{m,n}}^a \frac{\mu(0)}{\mu(r)} \frac{dr}{r} \tag{59}$$

III. ASYMPTOTIC REGIMES FOR SLOWING DOWN VIA VESSEL EDDY CURRENTS

A. Introduction

Three separate asymptotic regimes for the slowing down of dynamo mode rotation via eddy currents induced in a resistive vacuum vessel can be identified from the preceding analysis. These regimes, which correspond to different orderings for the intrinsic mode rotation parameter $\lambda_{(0)}^{m,n}$ [see Eq. (55)], are discussed in the following.

B. The ultra-thin-shell regime

The ultra-thin-shell regime corresponds to the ordering $\lambda_{(0)}^{m,n} \ll 1$,

in which either the intrinsic plasma rotation is very low or the vacuum vessel is extremely thin. In this regime, there is virtually no shielding of the tearing perturbation by the vacuum vessel: i.e., the perturbation amplitude remains significant in the region $b < r < c$. In this case, the torque balance equation (54) reduces to

$$\hat{\Omega}_s \approx \frac{1}{1 + (b_s^{m,n} / \Lambda B_0)^2}, \tag{61}$$

where

$$\hat{\Omega}_s = \frac{\Omega_s}{\Omega_s^{(0)}} \tag{62}$$

is the normalized dynamo mode rotation velocity. It can be seen that the mode rotation decreases smoothly and monotonically as the mode amplitude $b_s^{m,n}$ is increased. The rotation is significantly reduced (compared to its value in the absence of vacuum vessel eddy currents) whenever

$$b_s^{m,n} \gg \Lambda B_0. \tag{63}$$

C. The thin-shell regime

The thin-shell regime corresponds to the ordering $1 \ll \lambda_{(0)}^{m,n} \ll \lambda_c^{m,n}$.

In this regime, there is strong shielding of the tearing perturbation by the vacuum vessel: i.e., the perturbation amplitude is insignificant in the region $b < r < c$. Nevertheless, the basic thin-shell approximation ordering $n\Omega_s \tau_b \ll b / \delta_b$ still holds. In this case, the torque balance equation (54) reduces to

$$\hat{\Omega}_s \approx \frac{1}{2} + \frac{1}{2} \sqrt{1 - (b_s^{m,n} / \Lambda' B_0)^2}, \tag{65}$$

where

$$\Lambda' = \frac{\lambda_{(0)}^{m,n} \Lambda}{2} = \left[\frac{\tau_H^2 \tau_b (n\Omega_s^{(0)})^2}{2 \tau_V} \frac{m^2 + n^2 \epsilon_s^2}{n^2 \epsilon_s^2} \frac{1}{E_{sb}^{m,n} E_{bs}^{m,n}} \right]^{1/2} \int_{r_s^{m,n}}^a \frac{\mu(0)}{\mu(r)} \frac{dr}{r} \tag{66}$$

Note that when $b_s^{m,n}$ exceeds the critical value $\Lambda' B_0$, the mode bifurcates to a slowly rotating state characterized by $\Omega_s \tau_b \sim O(1)$. This bifurcation is irreversible, in the sense that $b_s^{m,n}$ must be reduced substantially before the reverse bifurcation takes place. Thus, the mode rotation is effectively arrested whenever

$$b_s^{m,n} > \Lambda' B_0. \tag{67}$$

Note that bifurcations only occur for²¹

$$\lambda_{(0)}^{m,n} > 3\sqrt{3} = 5.196. \tag{68}$$

D. The thick-shell regime

The thick-shell regime corresponds to the ordering

$$\lambda_c^{m,n} \ll \lambda_{(0)}^{m,n}. \tag{69}$$

In this regime, there is very strong shielding of the tearing perturbation by the vacuum vessel: i.e., the perturbation amplitude is zero in the region $b < r < c$. The dispersion relation of the shell, Eq. (40), is replaced by²²

$$\Delta \Psi_b^{m,n} = \left(in\Omega_s \tau_b \frac{b}{\delta_b} \right)^{1/2} \Psi_b^{m,n}. \tag{70}$$

It follows that

$$\Delta \Psi_s^{m,n} \approx e^{-i\pi/4} \frac{E_{sb}^{m,n} E_{bs}^{m,n}}{(n\Omega_s \tau_b b / \delta_b)^{1/2}} \Psi_s^{m,n}. \tag{71}$$

Hence,

$$\delta T_{\phi EM}^{m,n} \approx - \frac{\sqrt{2} \pi^2 R_0}{\mu_0} \frac{n |\Psi_s^{m,n}|^2}{m^2 + n^2 \epsilon_s^2} \frac{E_{sb}^{m,n} E_{bs}^{m,n}}{(n\Omega_s \tau_b b / \delta_b)^{1/2}}. \tag{72}$$

Torque balance yields

$$\frac{\sqrt{27}}{2} \hat{\Omega}_s^{1/2} (1 - \hat{\Omega}_s) = \left(\frac{b_s^{m,n}}{\Lambda'' B_0} \right)^2, \tag{73}$$

where

$$\Lambda'' = \left[\frac{4\sqrt{2}}{\sqrt{27}} \frac{\tau_H^2 (n\Omega_s^{(0)})^{3/2} (\tau_b b / \delta_b)^{1/2}}{\tau_V} \frac{m^2 + n^2 \epsilon_s^2}{n^2 \epsilon_s^2} \right]^{1/2} \times \frac{1}{E_{sb}^{m,n} E_{bs}^{m,n}} \int_{r_s^{m,n}}^a \frac{\mu(0)}{\mu(r)} \frac{dr}{r} \tag{74}$$

Note that when $b_s^{m,n}$ exceeds the critical value $\Lambda'' B_0$, the mode bifurcates to a slowly rotating state characterized by $\Omega_s \tau_b \sim O(1)$. This bifurcation is irreversible, in the sense that $b_s^{m,n}$ must be reduced substantially before the reverse bifurcation takes place. Thus, the mode rotation is effectively arrested whenever

$$b_s^{m,n} > \Lambda'' B_0. \quad (75)$$

IV. ESTIMATE OF CRITICAL PLASMA PARAMETERS

A. Introduction

In order to proceed further, it is necessary to estimate a number of critical plasma parameters which cannot be directly measured on MST or RFX.

B. Estimate of the mode rotation velocity

In the preceding analysis, the parameter $\Omega_s^{(0)}$ represents the toroidal angular phase velocity of a typical dynamo mode in the absence of vacuum vessel eddy currents. Of course, this quantity can be measured directly in MST, where it is found that²³

$$u_\phi^{(0)} = R_0 \Omega_s^{(0)} \approx 10 \text{ km s}^{-1}. \quad (76)$$

Unfortunately, it is impossible to measure $\Omega_s^{(0)}$ on RFX, since dynamo modes are never observed to rotate in this device. It is, therefore, necessary to estimate what the typical toroidal angular phase velocity of dynamo modes would be on RFX in the absence of slowing down torques due to vacuum vessel eddy currents.

Theoretically, $u_\phi^{(0)}$ is expected to be the sum of the toroidal $\mathbf{E} \wedge \mathbf{B}$ and electron diamagnetic velocities evaluated in the plasma core.²⁴ However, an RFP is characterized by a stochastic magnetic core generated by overlapping dynamo modes. The stochastic core gives rise to the development of an ambipolar electric field which reduces outward radial electron transport along magnetic field lines to the level of the corresponding ion transport. The $\mathbf{E} \wedge \mathbf{B}$ velocity associated with this electric field scales like an electron diamagnetic velocity.²⁵ It follows that $u_\phi^{(0)}$ should also scale as an electron diamagnetic velocity, giving

$$n \Omega_s^{(0)} \approx 6 \frac{m T_{e0} (\text{eV})}{a^2 B_0}. \quad (77)$$

Here, T_{e0} is the central electron temperature. The factor 6 is necessary in order to ensure that the above formula yields $u_\phi^{(0)} \approx 10 \text{ km s}^{-1}$ for typical MST parameters.

C. Estimate of the plasma viscosity

Plasma viscosity is not usually directly measured in RFPs. It is, therefore, necessary to estimate the plasma viscosity in terms of quantities which are measured.

Suppose that the plasma viscosity profile takes the form

$$\mu(r) = \begin{cases} \infty & r < r_c \\ \mu_c & r_c \leq r \leq a \end{cases} \quad (78)$$

In other words, there is zero momentum confinement in the stochastic core, $r < r_c$, and the viscosity is approximately constant in the outer regions of the plasma. Suppose, further, that the intrinsic plasma rotation at the edge is negligibly small [i.e., $\Omega^{(0)}(a) \approx 0$] and that all of the toroidal momentum input to the plasma takes place inside the core. In this case, it is easily demonstrated that

$$\Omega^{(0)}(r) = \Omega_c^{(0)} \begin{cases} 1 & r < r_c \\ \ln(r/a)/\ln(r_c/a) & r_c \leq r \leq a \end{cases} \quad (79)$$

In other words, the plasma rotation is uniform in the stochastic core, and highly sheared in the outer regions of the plasma.

The viscous diffusion time scale (58) is conveniently redefined

$$\tau_V = \frac{\rho_0 a^2}{\mu_c}. \quad (80)$$

Suppose that the plasma density profile is approximately uniform. It follows that the momentum confinement time τ_M (defined as the ratio of the net plasma toroidal angular momentum to the toroidal angular momentum injection rate) is related to τ_V via

$$\tau_V = - \frac{a^3 d\Omega^{(0)}(a)/dr}{\int_0^a \Omega^{(0)} r dr} \tau_M. \quad (81)$$

Hence,

$$\tau_V = \frac{4 \tau_M}{1 - (r_c/a)^2}. \quad (82)$$

In this paper, it is assumed that

$$\tau_M \approx \tau_E, \quad (83)$$

where τ_E is the energy confinement time (which is measured in both MST and RFX). This is a plausible assumption, since whenever τ_M has been measured in toroidal fusion devices it has been found to be very similar in magnitude to τ_E .^{26,27} It follows that

$$\tau_V \int_{r_s}^a \frac{\mu(0)}{\mu(a)} \frac{dr}{r} \rightarrow \kappa \tau_E \quad (84)$$

in Eqs. (59), (66), and (74), where

$$\kappa = \frac{4 \ln(a/r_c)}{1 - (r_c/a)^2}. \quad (85)$$

V. SLOWING DOWN CALCULATIONS

A. The Madison Symmetric Torus

In MST, the plasma is surrounded by a single 5 cm thick aluminum (alloy 6061-T6) shell which simultaneously plays the role of the vacuum vessel and the stabilizing shell. Since there is no perfectly conducting shell surrounding this finite resistivity shell, the parameter c takes the value ∞ (i.e., the perfectly conducting shell of the preceding analysis is located infinitely far away from the plasma). The typical shell and plasma parameters for MST⁶ are listed in Table I. It follows that

$$\tau_H = \frac{\sqrt{\mu_0 m_p n_{e0}} a}{B_0} = 5.5 \times 10^{-7} \text{ s}, \quad (86)$$

$$n \Omega_s^{(0)} = 6 \frac{T_{e0} (\text{eV})}{a^2 B_0} = 4.0 \times 10^4 \text{ rad s}^{-1}, \quad (87)$$

$$\tau_b = \mu_0 \sigma_b \delta_b b = 0.82 \text{ s}. \quad (88)$$

TABLE I. Typical MST parameters.

Parameter	Units	Symbol	Value
Major radius	m	R_0	1.5
Plasma minor radius	m	a	0.51
Toroidal plasma current	kA	I_ϕ	340
Equilibrium magnetic field strength	T	$B_0 \equiv B_\theta(a) = \mu_0 I_\phi / 2\pi a$	0.13
Central electron temperature	eV	T_{e0}	230
Central electron number density	m^{-3}	n_{e0}	1×10^{19}
Energy confinement time	ms	τ_E	1
Vacuum vessel minor radius	m	b	0.52
Vacuum vessel thickness	cm	δ_b	5
Vacuum vessel resistivity	Ωm	$1/\sigma_b$	4.0×10^{-8}

The typical equilibrium parameters for MST are $\epsilon_a = 0.34$, $\alpha = 3.0$, $\Theta_0 = 1.71$, $F = -0.2$, and $\Theta = 1.59$. Here, we have adopted a somewhat low value of α in order to compensate for the absence of pressure in our model (the final result turns out to be fairly insensitive to this parameter). The characteristic dynamo mode for this equilibrium is the $m = 1$, $n = 6$ mode. It is easily demonstrated that $r_s^{1,6} = 0.3381a$, so that $n\epsilon_s = 0.69$. Furthermore, Newcomb's equation can be solved to give

$$E^{1,6}(b) = 1.038, \tag{89}$$

$$E^{1,6}(c) = 17.59, \tag{90}$$

$$E_{bs}^{1,6} = 5.826, \tag{91}$$

$$E_{sb}^{1,6} = 1.614. \tag{92}$$

Finally, the radius of the stochastic plasma core is taken to be $r_c = 0.7a$, yielding

$$\kappa = \frac{4 \ln(a/r_c)}{1 - (r_c/a)^2} = 2.8. \tag{93}$$

The parameters $\lambda_{(0)}^{1,6}$ and $\lambda_c^{1,6}$ take the values

$$\lambda_{(0)}^{1,6} = \frac{n\Omega_s^{(0)}\tau_b[E^{1,6}(c) - E^{1,6}(b)]}{E_{sb}^{1,6}E_{bs}^{1,6}} = 5.7 \times 10^4, \tag{94}$$

and

$$\lambda_c^{1,6} = \frac{b [E^{1,6}(c) - E^{1,6}(b)]}{\delta_b E_{sb}^{1,6}E_{bs}^{1,6}} = 18.3, \tag{95}$$

respectively. It can be seen that

$$\lambda_c^{1,6} \ll \lambda_{(0)}^{1,6} \tag{96}$$

in MST. Thus, the thick-shell regime, discussed in Sec. III D, is applicable. It follows that the eddy currents which slow down the rotation of the 1,6 mode do not penetrate the aluminum shell, but are, instead, radially localized within a skin-depth of its inner boundary.

According to Eq. (73), the relationship between the mode amplitude parameter $b_s^{1,6}$ and the normalized mode rotation parameter $\hat{\Omega}_s$ in MST is

$$\frac{\sqrt{27}}{2} \hat{\Omega}_s^{1/2} (1 - \hat{\Omega}_s) = \left(\frac{b_s^{1,6}}{\Lambda'' B_0} \right)^2, \tag{97}$$

where

$$\Lambda'' = \left[\frac{4\sqrt{2}}{\sqrt{27}\kappa} \frac{\tau_H^2 (n\Omega_s^{(0)})^{3/2} (\tau_b b / \delta_b)^{1/2}}{\tau_E} \frac{m^2 + n^2 \epsilon_s^2}{n^2 \epsilon_s^2} \frac{1}{E_{sb}^{1,6} E_{bs}^{1,6}} \right]^{1/2} = 3.0 \times 10^{-2}. \tag{98}$$

The parameter $b_s^{m,n}$ can be related to the nominal m, n magnetic island width $W_s^{m,n}$ via

$$\frac{W_s^{m,n}}{a} = 4 \left[\frac{r_s^{m,n}}{a} \frac{b_s^{m,n}}{(F_s^{m,n})' B_0} \right]^{1/2}, \tag{99}$$

where

$$(F_s^{m,n})' = \frac{a}{B_0} \left[\frac{d(mB_\theta - n\epsilon B_\phi)}{dr} \right]_{r_s^{m,n}}. \tag{100}$$

It is easily demonstrated that $(F_s^{1,6})' = 1.44$ for the equilibrium in question. Thus, $W_s^{1,6}/a = 1.94(b_s^{1,6}/B_0)^{1/2}$. Furthermore, in the thick-shell regime the amplitudes of the perturbed poloidal and toroidal magnetic fields just inside the aluminum shell (which is where the Mirnov coils are located in MST) are related to $b_s^{m,n}$ via

$$b_{\theta b}^{m,n} = \frac{m}{m^2 + n^2 \epsilon_b^2} E_{bs}^{m,n} b_s^{m,n}, \tag{101}$$

$$b_{\phi b}^{m,n} = \frac{n \epsilon_b}{m^2 + n^2 \epsilon_b^2} E_{bs}^{m,n} b_s^{m,n}. \tag{102}$$

Hence, $b_{\theta b}^{1,6} = 1.09 b_s^{1,6}$ and $b_{\phi b}^{1,6} = 2.28 b_s^{1,6}$.

B. The reversed field experiment

In RFX, the plasma is surrounded by a high resistivity, inconel (alloy 625) vacuum vessel which is, in turn, surrounded by a 6.5 cm thick aluminum (alloy 6061-T6) shell. In the following, we ignore the resistivity of the aluminum shell compared to that of the vacuum vessel. In other words, the aluminum shell is treated as a perfect conductor. The typical shell and plasma parameters for RFX⁷ are listed in Table II. The chosen values for the effective thickness and the effective resistivity of the vacuum vessel are justified in the appendix. It follows that

$$\tau_H = \frac{\sqrt{\mu_0 m_p n_{e0}} a}{B_0} = 4.0 \times 10^{-7} \text{ s}, \tag{103}$$

TABLE II. Typical RFX parameters.

Parameter	Units	Symbol	Value
Major radius	m	R_0	2.0
Plasma minor radius	m	a	0.457
Toroidal plasma current	kA	I_ϕ	600
Equilibrium magnetic field strength	T	$B_0 \equiv B_\theta(a) = \mu_0 I_\phi / 2\pi a$	0.26
Central electron temperature	eV	T_{e0}	230
Central electron number density	m^{-3}	n_{e0}	2×10^{19}
Energy confinement time	ms	τ_E	1
Vacuum vessel minor radius	m	b	0.490
Vacuum vessel (effective) thickness	mm	δ_b	3.5
Vacuum vessel (effective) resistivity	Ωm	$1/\sigma_b$	64.7×10^{-8}
Stabilizing shell minor radius	m	c	0.535
Stabilizing shell thickness	cm	δ_c	6.5
Stabilizing shell resistivity	Ωm	$1/\sigma_c$	4.4×10^{-8}

$$n\Omega_s^{(0)} = 6 \frac{T_{e0}(\text{eV})}{a^2 B_0} = 2.5 \times 10^4 \text{ rad s}^{-1}, \quad (104)$$

$$\tau_b = \mu_0 \sigma_b \delta_b b = 3.3 \times 10^{-3} \text{ s}. \quad (105)$$

The typical equilibrium parameters for RFX are $\epsilon_a = 0.23$, $\alpha = 3.5$, $\Theta_0 = 1.65$, $F = -0.2$, and $\Theta = 1.56$. Here, we have again adopted a somewhat low value of α in order to compensate for the absence of pressure in our model. The characteristic dynamo mode for this equilibrium is the $m = 1$, $n = 9$ mode. It is easily demonstrated that $r_s^{1,9} = 0.384a$, so that $n\epsilon_s = 0.79$. Furthermore, Newcomb's equation can be solved to give

$$E^{1,9}(b) = 0.433, \quad (106)$$

$$E^{1,9}(c) = 1.258, \quad (107)$$

$$E_{bs}^{1,9} = 5.467, \quad (108)$$

$$E_{sb}^{1,9} = 1.513. \quad (109)$$

Finally, the radius of the stochastic plasma core is again taken to be $r_c = 0.7a$, yielding $\kappa = 2.8$.

The parameters $\lambda_{(0)}^{1,9}$ and $\lambda_c^{1,9}$ take the values

$$\lambda_{(0)}^{1,9} = \frac{n\Omega_s^{(0)} \tau_b [E^{1,9}(c) - E^{1,9}(b)]}{E_{sb}^{1,9} E_{bs}^{1,9}} = 8.36, \quad (110)$$

and

$$\lambda_c^{1,9} = \frac{b [E^{1,9}(c) - E^{1,9}(b)]}{\delta_b E_{sb}^{1,9} E_{bs}^{1,9}} = 14.0, \quad (111)$$

respectively. Note that

$$1 \ll \lambda_{(0)}^{1,9} \ll \lambda_c^{1,9}, \quad (112)$$

so the thin-shell regime, discussed in Sec. III, is applicable.

According to Eq. (54), the relationship between the mode amplitude parameter $b_s^{1,9}$ and the normalized mode rotation parameter $\hat{\Omega}_s$ in RFX is

$$\frac{(1 - \hat{\Omega}_s)[1 + (8.36\hat{\Omega}_s)^2]}{\hat{\Omega}_s} = \left(\frac{b_s^{1,9}}{\Lambda B_0} \right)^2, \quad (113)$$

where

$$\Lambda = \left[\frac{2}{\kappa} \frac{\tau_H^2}{\tau_b \tau_E} \frac{m^2 + n^2 \epsilon_s^2}{n^2 \epsilon_s^2} \frac{E_{sb}^{1,9} E_{bs}^{1,9}}{[E^{1,9}(c) - E^{1,9}(b)]^2} \right]^{1/2} = 1.0 \times 10^{-3}. \quad (114)$$

It is easily demonstrated that $(F_s^{1,9})' = 1.73$ for the equilibrium in question. Thus, $W_s^{1,9}/a = 1.88(b_s^{1,9}/B_0)^{1/2}$, where use has been made of Eq. (99). Furthermore, since the thin-shell approximation is valid, the amplitudes of the perturbed poloidal and toroidal magnetic fields just inside the aluminum shell (which is where the Mirnov coils are located in RFX) are related to $b_s^{m,n}$ via

$$b_{\theta c}^{m,n} = \frac{m}{m^2 + n^2 \epsilon_c^2} \frac{E_{cs}^{m,n}}{[1 + (\lambda^{m,n})^2]^{1/2}} b_s^{m,n}, \quad (115)$$

$$b_{\phi c}^{m,n} = \frac{n \epsilon_c}{m^2 + n^2 \epsilon_c^2} \frac{E_{cs}^{m,n}}{[1 + (\lambda^{m,n})^2]^{1/2}} b_s^{m,n}, \quad (116)$$

where

$$E_{cs}^{m,n} = \frac{\hat{\psi}_s^{m,n}(a, c)(m^2 + n^2 \epsilon_c^2)}{k_m(n\epsilon_c) i_m(n\epsilon_a) - k_m(n\epsilon_a) i_m(n\epsilon_c)}. \quad (117)$$

Now, $E_{cs}^{1,9} = 6.625$ for the equilibrium in question, so

$$b_{\theta c}^{1,9} = \frac{0.975 b_s^{1,9}}{[1 + (8.36\hat{\Omega}_s)^2]^{1/2}}, \quad (118)$$

$$b_{\phi c}^{1,9} = \frac{2.15 b_s^{1,9}}{[1 + (8.36\hat{\Omega}_s)^2]^{1/2}}. \quad (119)$$

C. Results

Figure 4 shows the toroidal angular phase velocity Ω_s of the characteristic dynamo mode plotted as a function of the associated saturated island width W_s at the rational surface for both MST and RFX. Note that the characteristic mode is the 1,6 mode for the case of MST and the 1,9 mode for the case of RFX.

For the case of MST, it can be seen that as the saturated island width is gradually increased, the phase velocity of the characteristic mode is gradually reduced via the action of eddy currents excited in the vacuum vessel. Note, however,

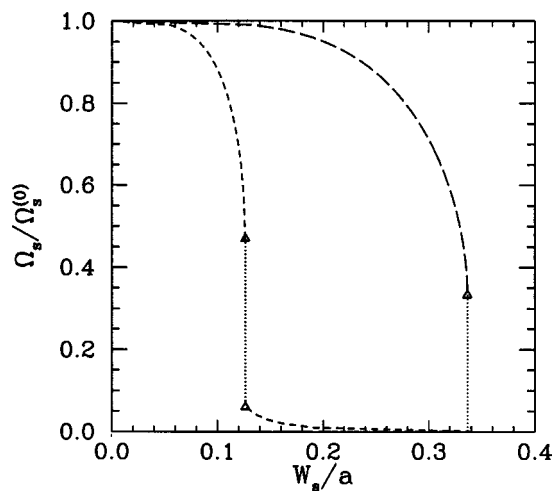


FIG. 4. The toroidal angular phase velocity Ω_s of the characteristic dynamo mode (normalized to the corresponding velocity $\Omega_s^{(0)}$ in the absence of vacuum vessel eddy currents) as a function of the associated saturated island width W_s (normalized with respect to the minor radius of the plasma a) calculated for MST (long-dashed line) and RFX (short-dashed line).

that if the phase velocity falls below a certain critical value, corresponding to one-third of its value in the absence of eddy currents, then a bifurcation to a branch of solutions on which the mode is effectively nonrotating is triggered. The bifurcation point is indicated by a triangle in Fig. 4. Likewise, the bifurcation path (from the rotating to the nonrotating branch of solutions) is shown as a dotted line. The bifurcation is irreversible: i.e., once the mode has made the transition to the nonrotating branch of solutions the saturated island width must be reduced substantially before the reverse transition takes place.

For the case of RFX, it can be seen that as the saturated island width is gradually increased the phase velocity of the characteristic mode is gradually reduced via the action of eddy currents excited in the vacuum vessel. Note, however, that this reduction in phase velocity takes place far more rapidly, and at significantly lower values of the saturated island width, than in MST. This is largely due to the fact that the RFX vacuum vessel is much more resistive than the MST vessel. As before, if the phase velocity falls below a certain critical value, corresponding to 0.47 of its value in the absence of eddy currents, then a bifurcation to a slowly rotating branch of solutions is triggered. The bifurcation points are indicated by triangles in Fig. 4. Likewise, the bifurcation path (from the rapidly to the slowly rotating branch of solutions) is shown as a dotted line. The bifurcation is irreversible, in the sense discussed above.

Now, the typical saturated island width of a dynamo mode in an RFP plasma is approximately 20% of the minor radius (see, for instance, Figs. 4 and 1 in Refs. 23 and 28, respectively). Note, from Fig. 4, that if $W_s/a \approx 0.2$ then our model predicts that dynamo mode rotation in MST is virtually unaffected by vacuum vessel eddy currents, whereas any mode rotation in RFX is essentially eliminated by such currents. This observation leads us to conjecture that the observed lack of mode rotation in RFX, compared to MST, is a

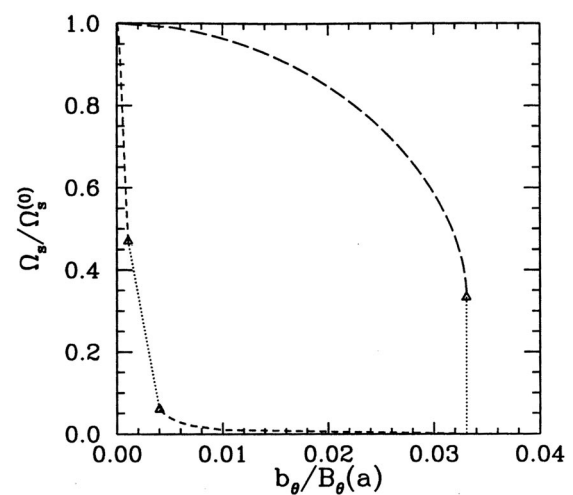


FIG. 5. The toroidal angular phase velocity Ω_s of the characteristic dynamo mode (normalized to the corresponding velocity $\Omega_s^{(0)}$ in the absence of vacuum vessel eddy currents) as a function of the associated perturbed poloidal magnetic field b_θ seen at the Mirnov coils [normalized with respect to the edge equilibrium magnetic field $B_\theta(a)$] calculated for MST (long-dashed line) and RFX (short-dashed line).

direct consequence of the eddy currents induced in the RFX vacuum vessel.

Figure 5 shows the toroidal angular phase velocity Ω_s of the characteristic dynamo mode plotted as a function of the associated perturbed poloidal magnetic field b_θ calculated at the radius of the Mirnov coils for both MST and RFX. It can be seen that rotation is predicted to collapse in MST when the ratio $b_\theta/B_\theta(a)$ exceeds about 3%. Since $B_\theta(a) \approx 1300$ gauss (see Table I), it follows that the critical value of b_θ needed to arrest the mode rotation in MST is about 40 gauss. This is a larger value than is generally observed in MST, except perhaps at sawtooth crashes. Thus, eddy current torques are almost certainly insignificant in MST during the sawtooth ramp phase, but may play a role in the sudden slowing down of mode rotation seen at sawtooth crashes.⁹ The mode rotation is predicted to collapse in RFX when the ratio $b_\theta/B_\theta(a)$ exceeds about 0.1%. Since $B_\theta(a) \approx 2600$ gauss (see Table II), it follows that the critical value of b_θ needed to arrest the mode rotation in RFX is about 3 gauss. This is a significantly smaller value than is generally observed in RFX,¹⁴ which lends further credence to our conjecture that vacuum vessel eddy currents are the primary cause of the lack of dynamo mode rotation in this device.

Figure 6 shows the toroidal angular phase velocity Ω_s of the characteristic dynamo mode plotted as a function of the associated perturbed toroidal magnetic field b_ϕ calculated at the radius of the Mirnov coils for both MST and RFX. Note that $b_\phi \sim 2b_\theta$ in both devices.

Preliminary calculations for TPE-RX indicate that the torque curve for this device lies between those for MST and RFX. In other words, the slowing down problem in TPE-RX is predicted to be significantly worse than that in MST, but not as bad as that in RFX, in accordance with experimental observations.

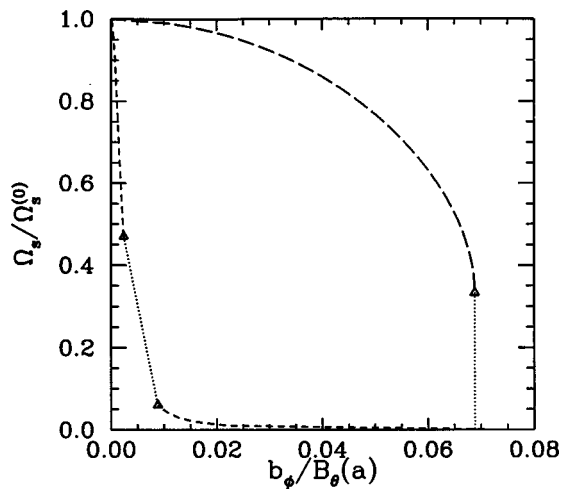


FIG. 6. The toroidal angular phase velocity Ω_s of the characteristic dynamo mode (normalized to the corresponding velocity $\Omega_s^{(0)}$ in the absence of vacuum vessel eddy currents) as a function of the associated perturbed toroidal magnetic field b_ϕ seen at the Mirnov coils [normalized with respect to the edge equilibrium magnetic field $B_\theta(a)$] calculated for MST (long-dashed line) and RFX (short-dashed line).

VI. SUMMARY

Locked (i.e., nonrotating) dynamo modes give rise to a serious edge loading problem during the operation of high current reversed field pinches. Rotating dynamo modes generally have a far more benign effect. Dynamo modes are usually observed to rotate in MST, whereas in RFX these modes remain locked throughout the duration of the plasma discharge. The locked dynamo modes in RFX are a cause for concern because they limit the maximum achievable plasma current.

An analytic model has been developed in order to investigate the slowing down effect of electromagnetic torques due to vacuum vessel eddy currents on the rotation of dynamo modes in both MST and RFX. Despite the model's simplicity, the results of our investigation are sufficiently clear-cut to enable us to conclude, with some degree of certainty, that vacuum vessel eddy currents are the primary cause of the observed lack of dynamo mode rotation in RFX. The corresponding eddy currents in MST are found to be too weak to cause a similar problem. The crucial difference between RFX and MST is the presence of a thin, highly resistive vacuum vessel in the former device. The MST vacuum vessel is thick and highly conducting.

VII. DISCUSSION

In the above, we have demonstrated, fairly conclusively, that vacuum vessel eddy currents are largely responsible for the severe locked mode problems encountered in RFX. Note, however, that such problems are likely to be generic to any large RFP equipped with a thin vacuum vessel. In the following, armed with this knowledge, we briefly examine four possible methods for alleviating locked mode problems in such RFPs. These methods are: (i) reducing the plasma current; (ii) decreasing the resistance of the vacuum vessel; (iii)

decreasing the radial extent of the interspace between the vacuum vessel and the stabilizing shell; and (iv) spinning the plasma using neutral beams.

Let us examine the scaling of the critical radial magnetic field at the rational surface $b_c^{m,n}$ (normalized with respect to the scale equilibrium field magnetic B_0), above which the rotation of the characteristic dynamo mode is significantly reduced, with the toroidal plasma current I_ϕ . It is assumed, for the sake of simplicity, that the plasma density and the various equilibrium plasma profiles remain constant as I_ϕ is varied. According to the well-known Connor–Taylor (constant beta) scaling law,²⁹ $T_{e0} \propto I_\phi$ and $\tau_E \propto I_\phi^{3/2}$. It follows that $B_0 \propto I_\phi$, $\tau_H \propto I_\phi^{-1}$, and $n\Omega_s^{(0)}$ is independent of I_ϕ . Furthermore, the intrinsic mode rotation parameter $\lambda_{(0)}^{m,n}$ is also independent of I_ϕ . RFX lies in the thin-shell regime discussed in Sec. III. It is easily demonstrated that $b_c^{m,n}/B_0 \propto I_\phi^{-7/4}$ in this limit. Other more empirical scaling laws (e.g., $\tau_E \propto I_\phi$) yield similar results. Thus, we predict a very strong inverse scaling of the critical mode amplitude required to cause locking of dynamo modes with increasing plasma current. It should certainly be possible to alleviate locked mode problems by operating at reduced plasma current. Conversely, locked mode problems can be expected to worsen dramatically as the plasma current is increased.

Let us examine the scaling of $b_c^{m,n}/B_0$ with the toroidal resistivity R_ϕ of the vacuum vessel. It is assumed, for the sake of simplicity, that all of the plasma parameters remain constant as R_ϕ is varied. It is also assumed that the poloidal resistivity R_θ of the vessel scales like R_ϕ . According to the analysis in Sec. III, at fixed plasma parameters the eddy current slowing down torque acting on the characteristic dynamo mode attains its maximum value when R_ϕ is such that the intrinsic plasma rotation parameter $\lambda_{(0)}^{m,n}$ [defined in Eq. (55)] is of order unity. Since $\lambda_{(0)}^{m,n} \simeq 8$ in RFX [see Eq. (110)], it is clear that the actual resistance of the RFX vacuum vessel is somewhat less than the value which maximizes the slowing down torque acting on dynamo modes. Thus, in principle, the severe locked mode problems in RFX could be alleviated by either making the vacuum vessel slightly more conducting or far more (i.e., by at least a factor 10) resistive. In practice, it is difficult to see how the RFX vacuum vessel could be made far more resistive: it is already fabricated out of very thin sheets of an extremely high resistivity material (i.e., inconel). On the other hand, the vessel could easily be made more conducting, either by increasing its thickness or fabricating it out of a less resistive material. In the thin-shell regime, it is easily demonstrated that $b_c^{m,n}/B_0 \propto R_\phi^{-1/2} \propto \tau_b^{1/2}$. Note the relatively weak scaling of $b_c^{m,n}/B_0$ with τ_b . This suggests that increasing the time constant τ_b of the vacuum vessel is not a particularly effective way of alleviating locked mode problems.

Let us examine the scaling of $b_c^{m,n}/B_0$ with the radial distance $d \equiv c - b$ between the thick stabilizing shell and the thin vacuum vessel. It is assumed, for the sake of simplicity, that all of the plasma parameters remain constant as d is varied. The spacing d between the two shells affects $b_c^{m,n}/B_0$ primarily through the term $E^{m,n}(c) - E^{m,n}(b)$, which appears in Eqs. (55) and (59). Let us assume, as seems reason-

able, that $E^{m,n}(c) - E^{m,n}(b) \propto d$ as $d \rightarrow 0$. RFX lies in the thin-shell regime discussed in Sec. III. Unfortunately, there is no dependence of $b_c^{m,n}/B_0$ on d in this regime (since the vacuum vessel fairly efficiently shields the tearing perturbation from the influence of the stabilizing shell in both the thin-shell and thick-shell regimes). This suggests that reducing the radial spacing between the vacuum vessel and the stabilizing shell is not an effective way of alleviating locked mode problems (unless the vacuum vessel is sufficiently thin and resistive to lie in the ultra-thin-shell regime).

Let us, finally, examine the scaling of $b_c^{m,n}/B_0$ with the intrinsic (i.e., that in the absence of vacuum vessel eddy currents) toroidal angular phase velocity $\Omega_s^{(0)}$ of the characteristic dynamo mode. It is assumed, for the sake of simplicity, that we can increase $\Omega_s^{(0)}$ via tangential neutral beam injection without substantially modifying any other plasma parameters. In the thin-shell regime, it is easily demonstrated that $b_c^{m,n}/B_0 \propto \Omega_s^{(0)}$. The relatively strong scaling of $b_c^{m,n}/B_0$ with increasing $\Omega_s^{(0)}$ suggests that spinning the plasma via tangential neutral beam injection is a fairly effective way of alleviating the locked mode problems. A crude estimate of the neutral beam power required to double $\Omega_s^{(0)}$ in RFX is

$$P_0 = \frac{M u_\phi V}{\kappa \tau_E}, \quad (120)$$

where $M \sim 3 \times 10^{-7}$ kg is the plasma mass, $u_\phi \sim 5$ km s⁻¹ is the intrinsic plasma toroidal velocity, V is the velocity of the injected particles, $\kappa = 2.8$, and $\tau_E \sim 10^{-3}$ s is the energy confinement time of the plasma. Now, $V \sim 3 \times 10^6$ m s⁻¹ for 50 keV hydrogen beams, giving $P_0 \sim 1.7$ MW. We conclude that at least 2 MW of neutral beam power would be required to significantly alleviate the locked mode problems in RFX.

ACKNOWLEDGMENTS

The authors would like to thank Professor S. C. Prager (University of Wisconsin, Madison) and Dr. S. Ortolani (Consorzio RFX, Padua) for helpful discussions during the preparation of this paper. This research was jointly funded by the U.S. Department of Energy, under Contract Nos. DE-FG05-96ER-54346 and DE-FG03-98ER-54504, and Consorzio RFX.

APPENDIX: THE RFX VACUUM VESSEL

The RFX vacuum vessel⁷ is fabricated out of inconel (alloy 625), and consists of a two-shell sandwich structure, with a 2 mm thick inner shell and a 1 mm thick outer shell connected together by a 0.5 mm thick corrugated sheet. In addition, there are 144 poloidal stiffening rings connecting the inner and outer shells. The spacing between the two shells is 3 cm. The calculated poloidal and toroidal resistances of the vessel are $R_\theta = 41 \times 10^{-6} \Omega$ and $R_\phi = 1.1 \times 10^{-3} \Omega$, respectively.⁷

According to Gimblett,²² the time constant of a shell whose resistivities differ in the poloidal and toroidal directions is given by

$$\tau_b = \mu_0 R_0 \frac{m^2 + n^2 \epsilon_b^2}{m^2 R_\phi + n^2 R_\theta}. \quad (A1)$$

For the case of the RFX vacuum vessel (with $m = 1$ and $n = 9$), we obtain $\tau_b = 3.33$ ms.

In this paper, we define the effective thickness of the RFX vacuum vessel to be $\delta_b = 3.5$ mm, which is the total thickness of the inconel which makes up the vessel over most of its area. It follows that the effective resistivity of the vessel is given by

$$\frac{1}{\sigma_b} = \frac{\mu_0 b \delta_b}{\tau_b} = 64.7 \times 10^{-8} \Omega \text{m}. \quad (A2)$$

Note that the effective resistivity is less than the actual resistivity of inconel ($128 \times 10^{-8} \Omega \text{m}$) in order to take account of the low resistance paths afforded by the poloidal stiffening rings.

¹J. A. Wesson and D. J. Campbell, *Tokamaks*, 2nd ed. (Clarendon, Oxford, 1998).

²H. A. B. Bodin, Nucl. Fusion **30**, 1717 (1990).

³J. B. Taylor, Phys. Rev. Lett. **33**, 1139 (1974).

⁴B. Alpher, M. K. Bevir, H. A. B. Bodin *et al.*, Plasma Phys. Controlled Fusion **31**, 205 (1989).

⁵S. Ortolani and D. D. Schnack, *Magnetohydrodynamics of Plasma Relaxation* (World Scientific, Singapore, 1993).

⁶R. N. Dexter, D. W. Kerst, T. W. Lovell, S. C. Prager, and J. C. Sprott, Fusion Technol. **19**, 131 (1991).

⁷F. Gnesotto, P. Sonato, W. R. Baker *et al.*, Fusion Eng. Des. **25**, 335 (1995).

⁸R. Fitzpatrick, "Formation and locking of the slinky mode in reversed field pinches," to appear in Phys. Plasmas.

⁹A. F. Almagri, S. Assasi, S. C. Prager, J. S. Sarff, and D. W. Kerst, Phys. Fluids B **4**, 4080 (1992).

¹⁰V. Antoni, L. Apolloni, M. Bagatin *et al.*, in *Plasma physics and controlled nuclear fusion 1994*, Proceedings 15th International Conference, Seville 1994 (International Atomic Energy Agency, Vienna, 1995), Vol. 2, p. 405.

¹¹T. Bolzonella, S. Ortolani, and J. S. Sarff, in *Controlled fusion and plasma physics*, Proceedings 25th European Conference, Prague 1998 (European Physical Society, Petit-Lancy, 1998), p. 789.

¹²Y. Yagi, S. Sekine, T. Shimada *et al.*, "Front-end system of the TPE-RX reversed field pinch machine," to appear in Fusion Eng. Des.

¹³Y. Yagi (private communication, 1988).

¹⁴S. Ortolani, (private communication, 1998).

¹⁵M. F. F. Nave and J. A. Wesson, Nucl. Fusion **30**, 2575 (1990).

¹⁶The standard large aspect-ratio ordering is $R_0/a \gg 1$, where R_0 and a are the major and minor radii of the plasma, respectively.

¹⁷The conventional definition of this parameter is $\beta = 2\mu_0 \langle p \rangle / \langle B^2 \rangle$, where $\langle \dots \rangle$ denotes a volume average, p is the plasma pressure, and B is the magnetic field strength.

¹⁸V. Antoni, D. Merlin, S. Ortolani, and R. Paccagnella, Nucl. Fusion **26**, 1711 (1986).

¹⁹W. A. Newcomb, Ann. Phys. (N.Y.) **10**, 232 (1960).

²⁰H. P. Furth, J. Killeen, and M. N. Rosenbluth, Phys. Fluids **6**, 459 (1963).

²¹R. Fitzpatrick, Nucl. Fusion **33**, 1049 (1993).

²²C. G. Gimblett, Nucl. Fusion **26**, 617 (1986).

²³D. J. Den Hartog, A. F. Almagri, J. T. Chapman *et al.*, Phys. Plasmas **2**, 2281 (1995).

²⁴G. Ara, B. Basu, B. Coppi, G. Laval, M. N. Rosenbluth, and B. V. Waddell, Ann. Phys. (N.Y.) **112**, 443 (1978).

²⁵M. R. Stoneking, S. A. Hokin, S. C. Prager, G. Fiksel, H. Ji, and D. J. Den Hartog, Phys. Rev. Lett. **73**, 549 (1994).

²⁶D. E. Post, K. Borrass, J. D. Callen *et al.*, in *ITER Physics*, ITER Document Series No. 21 (International Atomic Energy Agency, Vienna, 1991).

²⁷A. F. Almagri, J. T. Chapman, C. S. Chiang, D. Craig, D. J. Den Hartog, C. C. Hegna, and S. C. Prager, Phys. Plasmas **5**, 3982 (1998).

²⁸A. K. Hansen, A. F. Almagri, D. J. Den Hartog, S. C. Prager, and J. S. Sarff, Phys. Plasmas **5**, 2942 (1998).

²⁹J. W. Connor and J. B. Taylor, Phys. Fluids **27**, 2676 (1984).